

**Microglia contribute to excitatory synapse formation
in developing mouse neocortex**

Akiko Miyamoto

Doctor of Philosophy

**Department of Physiological Sciences
School of Life Science
The Graduate University for Advanced Studies**

2013

Contents

Abstract	3
Introduction	7
Materials and Methods.....	10
Results.....	22
Discussion	33
Acknowledgements	41
References	42
Figures.....	49

Abstract

It has been recently reported that microglia, the immune cells of the central nervous systems (CNS), actively interact with synapses in their resting state. Resting microglia selectively and physically contact synapses in the intact brain, and are also involved in synapse elimination in immature brain and in the penumbra region where the cortical area adjacent to ischemic core. This synapse elimination contributes to neural circuit reorganization during development, and likely also to circuit recovery from injury. However, although activated microglia can release several molecules related to synapse formation (e.g. thrombospondins (TSPs), neurotrophins), whether microglia can also actively contribute to synapse formation is not known. Therefore in this study, I focused on 1) whether microglia are involved in synapse formation in the intact mice neocortex during the developmental period of rapid increase in excitatory synapses (postnatal day (P) 8-10), and 2) the possible mechanisms of any such effect observed.

To elucidate whether microglia played any role in synaptogenesis in the developing neocortex, I needed to separately visualize and measure both microglia and neurons. I used Iba1-EGFP mice, in which enhanced green fluorescent protein (EGFP) is selectively expressed in microglia in the CNS. To visualize layer (L) 2/3 pyramidal neurons, I

performed *in utero* electroporation of embryonic day (E) 14-15 Iba1-EGFP mice with constructs which expressed red fluorescent protein. Using these mice, I could simultaneously observe microglia and neurons, and detect any contact or interactions between the two, using *in vivo* two-photon imaging under physiological conditions. During *in vivo* time-lapse imaging, the formation of dendritic protrusion was detected following microglia contact with dendrites. The formation rate of these protrusion was significantly higher in dendritic regions that had been contacted by microglia, as compared with adjacent dendritic regions (10 μm lateral) in which contacts had not generally been observed. Ninety percent of these newly formed protrusions have a filopodia structure. Although these filopodia sometimes retracted or disappeared during an imaging session, their overall survival rate was not significantly different from other newly formed filopodia. Real time imaging (with higher temporal resolution) revealed that the protrusions were usually formed very soon (< 10 minutes) after microglia contact. Thus, microglia contact with dendrites appears to be involved with initiation of filopodia.

I also observed microglia-neuron interactions at P12-14 and at P26-30. However, there was no significant difference about in the formation rate of filopodia between microglia contacted and adjacent dendritic regions, indicating the microglia associated filopodia formation was age-specific. It is known that microglia in the immature brain resemble

an active morphology. Injection of minocycline, which inhibits the activation of microglia, decreased microglia-induced filopodia formation. To investigate possible mechanisms mediating microglia-related spine formation, I checked TSP expression using immunohistochemistry and revealed that TSP1 was present in P8 microglia processes. Co-expression of TSP1 and EGFP (in Iba1-EGFP mice) was reduced at P14 and virtually absent in adult microglia. Confocal imaging was consistent with TSP1 possibly being present within the microglia themselves. Furthermore, multiple dosing of mice with gabapentin (GBP), a blocker of TSP1 receptor $\alpha 2\delta$ -1 subunit of voltage-dependent Ca^{2+} channel, significantly decreased filopodia formation. Together this data suggests that TSP1 is released from activated microglia and involved in the microglia-induced filopodia formation. Filopodia are known to be actin rich structures and I proposed that actin accumulation was needed for the structural re-arrangements accompanying filopodia formation. To visualize actin filaments, I cultured P5 cortical slices and transfected them with pCMV-lifeact-mCherry by ballistic gene transfer. Lifeact is a peptide that binds to actin. Real time imaging revealed that actin accumulated at the microglia contacted dendritic site, and filopodia formed at the peak of this actin accumulation. This suggests that microglia contact attracts the recruitment and formation of actin for filopodia formation.

Finally I investigated whether microglia contact mediated filopodia become functional synapses. Double transgenic mice were generated by crossing Iba1-tetracycline transactivator (Iba1-tTA) mice and tetracycline operator-diphtheria toxin A (tetO-DTA) mice. This enabled the selective ablation of microglia upon withdrawal of doxycycline (Dox) from the diet. The density of microglia was significantly decreased three days after of Dox removal, and spine density was significantly decreased by six days of Dox removal during P5-11. Minocycline injected mice had reduced spine density. Miniature excitatory postsynaptic currents (mEPSCs) were recorded from L2/3 pyramidal neurons, and mEPSCs frequency was significantly reduced in microglia ablated mice. These data indicate that microglia-induced filopodia mature into functional synapses during cortex development.

In conclusion, microglia contribute to excitatory synapse formation through filopodia formation at L2/3 pyramidal neurons in developmental mice neocortex. This indicated that microglia is contributed to not only neuronal circuit rearrangement but circuit formation.

Introduction

The establishment of precise synaptic connections is essential for the development of functional neural networks and appropriate brain development, plasticity and function.

In the mammalian central nervous systems, the number of excitatory synapses undergoes a rapid increase to reach a peak during neonatal development (Felipe et al., 1997; Elston et al., 2009). In layer 2/3 (L2/3) of mouse barrel cortex, this period of rapid synapse formation begins at postnatal day (P) 8 (Felipe et al., 1997) and also the major ascending projection in the barrel cortex, connecting L4 to L2/3 develops started at P8 (Bender et al., 2006). Over a corresponding period, postsynaptic dendrites develop filopodia, protrusions with a high motility that are thought to be precursors of spine, which form postsynaptic structure of excitatory synapse (Ziv and Smith, 1996; Fiala et al., 1998). Filopodia generation and spine formation also occurs rapidly during this same period of synapse formation (Lendvai et al., 2000). However the mechanisms of this rapid spine formation are unknown.

Microglia are immunocompetent cells that make up 10% of all cells in the central nervous systems (CNS) and can respond to brain infections and damage by undergoing “activation” and subsequent phagocytosis of neuronal debris. Recent research has

focused on their role in synapse rearrangements in the non-injured CNS. In the normal adult brain, resting (ramified) microglia have highly branched processes (Nimmerjahn et al., 2005) and frequently contact pre- and post-synaptic structures (Wake et al., 2009). In the ischemic brain, resting microglia are involved in synapse elimination in the cortical area adjacent to the ischemic core, where synapse elimination is enhanced (Wake et al., 2009). In the developing CNS, microglia are also involved in synapse elimination (Tremblay et al., 2010; Paolicelli et al., 2011; Schafer et al., 2012). Tremblay et al. (2010) showed that spines that had made contacts with microglia were frequently eliminated during the critical period in the visual cortex (Tremblay et al., 2010).

During neonatal cortical development, microglia rapidly increase in number and show a morphological phenotype similar to the activated amoeboid state, rather than the ramified “resting” state (Dalmau et al., 2003). Activated microglia are known to release a variety of molecules that can affect synapse formation, such as neurotrophins and thrombospondins (TSPs) (Chamak et al., 1994; Coull et al., 2005). Hence it is possible that microglia may play an active role in synapse formation, in addition to the better known role in synapse elimination. Lenz et al. (2013) provided some suggestive evidence for this in a neuronal culture model. They showed that estradiol application to co-cultures of preoptic neurons and microglia increased the number of spine-like structures.

This synaptogenesis effect was absent when estradiol was applied to pure neuronal cultures without microglia, suggesting that activated microglia somehow participated critically in this formation of spine-like protrusion (Lenz et al., 2013). However whether this occurs *in vivo*, and the way in which microglia may contribute to synapse formation has not been examined.

Therefore, in this study I aimed to investigate whether microglia are involved in spine formation during the early postnatal development in the mouse neocortex. Using *in vivo* two-photon imaging, I observed that filopodia were formed on L2/3 pyramidal neuron dendrites following microglia contact. Inhibition of microglia via pharmacological and genetic means decreased cortical spine density and a reduced frequency of spontaneous synaptic events. I further investigated the mechanisms of microglia-induced spinogenesis, revealing a role for TSP1 and actin filament accumulation. Together my results provide direct evidence that microglia can initiate spine formation in the developing brain. This is the new mechanisms of spinogenesis and microglia contributed not only to neuronal circuit rearrangement but also to circuit formation.

Materials and Methods

All animal experiments were approved by the Animal Research Committee of the National Institutes of Natural Sciences.

Animals

To visualize microglia, I used the Iba1-EGFP transgenic mouse, which expresses enhanced green fluorescent protein (EGFP) under the control of the ionized Ca^{2+} binding adapter molecule 1 (Iba1) promoter, which is a specific promoter in microglia and macrophages (Hirasawa et al., 2005). For microglia ablation experiments, double transgenic mice were generated by crossing Iba1-tetracycline transactivator (Iba1-tTA) mice (Tanaka et al., 2012) and tetracycline operator-diphtheria toxin A (tetO-DTA) mice (Stanger et al., 2007). Withdrawal of doxycycline (Dox) in the feed of these mice, leads to expression of the diphtheria toxin A (DTA) in mice expressing tTA (i.e. in microglia). Transgene induction was inhibited until DTA expression was needed by rearing mice with Dox 0.1 g/kg containing feed. All of the mice using the tetO system derived from a mixed background of C57BL/6 and 129Sv/Tac strains.

***In utero* electroporation**

To visualize L2/3 pyramidal neurons, I performed *in utero* electroporation of embryos at E14-15 in pregnant mice (Sehara et al., 2010). Pregnant mice were anesthetized with isoflurane (1.7 $\mu\text{l}/\text{min}$) during surgery. The uterus was exposed and approximately 1.5 μl of plasmid solution was injected into the lateral ventricle of each embryo using a glass pipette (tip diameter: 50-100 μm). The head of a single embryo was then put between tweezer-type electrodes, with 5 mm diameter tips (CUY650-P5; NEPA Gene, Chiba, Japan), and square electric pulses (35 V; 50 ms) were applied to the electrodes 5 times, at 950 ms intervals, using an electroporator (CUY21E; NEPA Gene). After the electric stimulus, embryos were quickly returned to the abdomen and the peritoneal membrane was sutured back together. The mother's skin was bound by clips (12032-07, Muromachi Kikai, Tokyo, Japan) to avoid reopening the surgical wound.

To enable sparse labelling of L2/3 pyramidal neurons, I used a plasmid which contained floxed red fluorescent protein (RFP; either pCALNL-DsRed-express (Addgene, Cambridge MA, US) or pCALNL-tdTomato; at 0.4 $\mu\text{g}/\mu\text{l}$), which was co-injected with a plasmid carrying Cre recombinase (pCAG-Cre (Addgene), 0.01 $\mu\text{g}/\mu\text{l}$). To check whether injection was success or not, Fast Green FCF 0.25 $\mu\text{g}/\mu\text{l}$ (F7258-25G, Sigma-aldrich, Tokyo, Japan) was also mixed in the plasmid solution.

***In vivo* two-photon imaging**

Electroporated Iba1-EGFP mice (P8-10) were anesthetized with urethane (1.7 g/kg body weight, intraperitoneal injection (i.p.)) and atropine (0.4 mg/kg, i.p.). Surgery and imaging were performed on a warming plate. After removal of the scalp, a cranial window (1.6 mm in diameter) was made over the primary somatosensory barrel cortex (1 mm posterior from Bregma and 2.5 mm lateral from the midline). A cover glass was put on to the cranial window and fixed with adhesive glue (Aron Alpha, Konishi, Osaka, Japan) and dental cement (Quick Resin, SHOFU, Kyoto, Japan). A custom-made imaging chamber was placed on to cranial window and the region above the cover glass was perfused with warm water (32-34 °C) during imaging.

Two-photon imaging was performed with a Ti:sapphire laser (Mai Tai HP, Spectra-Physics, Tokyo, Japan) operating at 960 nm wavelength. A laser scanning system (Olympus FLUOVIEW, Olympus, Tokyo, Japan) and an upright microscope (BX61WI, Olympus) with a water-immersion objective ($\times 25$, 1.05 NA, Olympus) was used for imaging acquisition. Fluorescence was separated by a 570 nm dichroic mirror with 495-550 nm (green channel: for EGFP fluorescence detection) and 570-630 nm (red channel: for DsRed-express or tdTomato fluorescence detection) emission filters, and detected by photomultipliers. For time lapse imaging, Z stack images (512×512 pixels, 0.099

$\mu\text{m}/\text{pixel}$, $0.5 \mu\text{m}$ Z-step) were taken every 5 minutes for between 30 minutes and 2 hours at a depth of 100 - 250 μm . For real time imaging, XYt images were taken every 1.6 seconds for 27 minutes.

Image analysis of microglia neuron interactions from time lapse imaging

Image stacks were visually inspected in ImageJ (National Institutes of Health, US) to determine colocation of GFP-labeled microglia and RFP-labeled dendrites. Detected regions of possible co-location were subsequently examined in greater detail at all image time points and Z sections to confirm possible contacts using ImageJ. To reduce noise, images were filtered with a 3×3 pixel median filter after background subtraction. The overlap between the red and the green channel was determined after thresholding the channels independently. Contacts between a microglia process and a labeled dendrite were determined only if the red and the green channel had overlapping pixels in at least two Z sections, and if the overlap consisted of a region that was at least twice the spatial resolution.

To define a dendritic protrusion (spine or filopodia), the structure had to be greater than $0.4 \mu\text{m}$ from the dendrite border. A spine refers to protrusions which have a head structure, while filopodia refer to protrusions which do not have head structures. This

categorization includes, stubby structures as filopodia. This is appropriate as these types of “spines” frequently disappear and are unstable, during development (Parnass et al., 2000). The formation rate of dendritic protrusions was calculated as the number of protrusions formed during or after contact, divided by the number of microglia contacts on a dendrite. Protrusions that appeared within 10 minutes of microglia contact onset were counted as protrusions formed by microglia contact. The formation rate of protrusions at dendritic regions 10 μm adjacent to the microglia contacted region were also counted, and used as a background (non-contacted) control comparison for the contacted regions.

For the pharmacological inhibition of microglia-induced filopodia formation, I used minocycline hydrochloride (M9511-1G, Sigma-aldrich) and gabapentin (G154-50MG, Sigma-aldrich).

Brain fixation and immunohistochemistry

Mice were deeply anesthetized with ketamine (0.13 mg/g, i.p.) and xylazine (0.01 mg/g, i.p.) and transcardially perfused with 4 % paraformaldehyde (PFA). The brain was dissected out, postfixed for 2 days in 4 % PFA at 4 °C and then 100 μm thick coronal slices that included the barrel cortex were sectioned with a vibratome (VT1000S; Leica,

Tokyo, Japan) to investigate microglia morphology (Iba1-EGFP mice) and spine density (electroporated Iba1-tTA::tetO-DTA or Iba1-tTA or wild C57BL/6 mice). Sections were mounted with VECTASHIELD mounting medium (H-100, Funakoshi, Tokyo, Japan) and imaging was performed within 7 days of sectioning.

30 μm thickness coronal sections containing barrel cortex were similarly cut for immunohistochemistry. Slices were incubated in blocking solution (0.1 % normal goat serum, 0.05 % NaN_3 , 0.5 % Triton X-100 in 0.1 M PBS) for 30 min. After washing with 0.1 M PBS, sections were incubated with primary antibodies (1:500 dilution; Anti-Iba1 antibody, 019-19741, Wako, Osaka, Japan) overnight at 4 °C. Then, slices were incubated with secondary antibodies (1:300 dilution; Alexa Fluor 633 Goat Anti-Rabbit, Life technologies, Carlsbad CA, US) overnight at 4 °C. Finally, sections were mounted with VECTASHIELD mounting medium with DAPI (H-1200, Funakoshi) and imaging was performed within 7 days.

For immunohistochemistry of TSP1, anti-TSP1 antibody (1:100 dilution; MA5-13398, Thermo Fisher Scientific K. K., Yokohama, Japan) was used as primary antibody, and Alexa Fluor 564 (1:2000 dilution; Mouse Anti-Mouse, Life technologies) was used as the secondary antibody.

Image Analysis for microglia morphology

Iba1-EGFP mice were used to visualize microglia, with fixed brain slices (as described above) of 100 μm thick slices were used to obtain the complete processes of microglia.

Confocal imaging was performed with a multi argon laser operating at a wavelength of 488 nm. A laser scanning system (Nikon A1, Nikon, Tokyo, Japan) and an inverted microscope with water-immersion objective ($\times 40$, 0.95 NA, Nikon) was used for imaging acquisition. Fluorescence was separated by a dichroic mirror with 495-550 nm (green channel: for EGFP fluorescence detection) emission filters and detected by photomultipliers. Z stack images (512×512 pixels, 0.198 $\mu\text{m}/\text{pixel}$, 0.5 μm Z-step) were taken for morphological analysis.

Image processing was performed using ImageJ software. Maximum intensity projections of Z-series stacks were created. For morphological analysis, the parameter of microglia process area was determined by circumscribing the area outlined by the ends of processes using the segmented line tool in ImageJ. Soma size was also calculated by circumscribing the cell body area using an intensity threshold in MetaMorph (Molecular devices, Tokyo, Japan). The number of microglia primary processes was manually counted, with primary processes defined as those starting from the microglia soma.

Image analysis for spine density

In utero electroporated mice were used for visualization of L2/3 pyramidal neuron dendritic spines. Brains were fixed and sectioned (100 μm) as described above. Confocal imaging was performed with 10 mW 561 nm solid laser. A laser scanning system (Nikon A1, Nikon) and an inverted microscope with a water-immersion objective ($\times 60$, 1.2 NA, Nikon) was used for imaging acquisition. Fluorescence was again separated by a dichroic mirror with 572-700 nm (red channel: for tdTomato fluorescence detection) emission filter, and detected by photomultipliers. Z stack images (512×512 pixels, 0.08 $\mu\text{m}/\text{pixel}$, 0.5 μm Z-step) were used to calculate of spine density.

Dendritic spines were identified in a series of Z-stack images and counted using ImageJ software. When dendritic spines were at too high density to readily identify individual spines, I used serial stack images to delineate individual spines. By scrolling through the stack of different optical sections, individual spines could be identified with greater certainty. All dendritic protrusions with a clearly recognizable stalk were counted as spines. Spine number was divided by the length of dendritic segment to generate dendritic spine density expressed as number/ μm .

Image analysis of TSP1 immunohistochemistry

Iba1-EGFP mice were used to visualize microglia and TSP1 immunohistochemistry. Brains were fixed, sectioned (30 μm) and stained as described above. Confocal images were obtained using a confocal laser microscope (Fluoview1000; Olympus) and an inverted microscope with oil-immersion objectives ($\times 40$, 1.30 NA, Olympus), and were digitized with Fluoview1000 software. A 488 nm Argon laser was used to excite of EGFP and a 543 nm laser was used to excite Alexa Fluor 564. The pinhole diameter was 80 μm and XY single plane images (1024 \times 1024 pixels, 0.31 μm /pixel) were taken for analysis. For the comparison of double-stained patterns, images were processed using Photoshop CS6 (Adobe Systems)

Slice culture and biolistic transfection

Cortical slice cultures were made from P5 Iba1-EGFP mice. After 1 days *in vitro* (DIV), cortical pyramidal neurons were transfected with a ballistic gene transfer gun using gold beads (4-6 mg) coated with 10 μg of the pCMV-lifeact-mCherry plasmid. Images were acquired at DIV 4 using a two-photon microscope with slice cultures perfused with warmed (32-34 $^{\circ}\text{C}$) artificial cerebral spinal fluid (ACSF), containing 126 mM NaCl, 2 mM KCl, 2 mM CaCl_2 , 24 mM NaHCO_3 , 1.2 mM NaH_2PO_4 , 1.3 mM MgSO_4 and 10 mM

glucose. Two-photon imaging was used 960 nm wave-length excitation, as described above for *in vivo* imaging. A water-immersion objective ($\times 25$, 1.05 NA, Olympus) was used for imaging acquisition. Fluorescence was separated by a 570 nm dichroic mirror with 495-550 nm (green channel: for EGFP fluorescence detection) and 570-630 nm (red channel: for mCherry fluorescence detection) emission filters, and detected by photomultipliers. Actin accumulation images were acquired using real time imaging at a single XY image plane acquired every 1.6 seconds for 27 minutes or every 5 seconds for 30 minutes.

The time course of microglia-dendrite contact, actin accumulation and filopodia formation was calculated using ImageJ. Microglia contact was defined as green fluorescent intensity that appeared on the dendrite. Aggregation of lifeact-mCherry was defined as the intensity of red fluorescence within the microglia contacted dendritic region. Filopodia formation was defined as the red fluorescence intensity protruding from the microglia contacted dendrite. The background intensity of image areas without any neuronal or microglia structures was subtracted from the intensity of the microglia and filopodia regions. The intensity of an adjacent region of the same dendrite without microglia contact or filopodia was used as background for the dendritic aggregation of lifeact-mCherry fluorescent signal. Fluorescence values were normalized by the

maximum intensity of each signal.

Electrophysiology

Acute brain slices were prepared from Iba1-tTA::tetO-DTA or Iba1-tTA mice at P12 following anaesthesia with ketamine (0.13 mg/g, i.p.) and xylazine (0.01 mg/g, i.p.), and transcardial perfusion with oxygenated (95%O₂/5%CO₂) slicing solution containing (in mM) : 230 sucrose, 26 NaHCO₃, 2 KCl, 1 MgCl₂, 1 KH₂PO₄, 0.5 CaCl₂, 10 glucose. Mice were decapitated and the brains were rapidly removed, and 350 µm thick coronal cortical slices were cut in cold slicing solution. Slices were stored in oxygenated ACSF (as described above for slice culture imaging) at 34°C for at least 45 min before being transferred to the recording chamber. Then they were continuously perfused with oxygenated recording ACSF and recordings were obtained at room temperature (around 25°C).

For mEPSCs recording, a slice was placed on the stage of an upright microscope and viewed with a ×40 water immersion objective. Whole-cell voltage-clamp recordings (at a holding potential of -70 mV) were made from the somata of visually identified barrel cortex L2/3 pyramidal neurons. Patch pipettes (5-8 MΩ) were constructed from borosilicate glass capillaries and filled with an internal solution containing (mM): 9 CsCl,

130 CH₃SO₃Cs, 2 EGTA, 10 HEPES, 4 Mg-ATP, 0.4 Na-GTP, pH adjusted to 7.3 with Tris.

During recording, 0.3 μM TTX and 10 μM SR95531 were continuously perfused to isolate mEPSC. Only cells with $R_{\text{series}} \leq 25 \text{ M}\Omega$ and $R_{\text{input}} \geq 200 \text{ M}\Omega$ were included for analysis, and no corrections for liquid junction potentials nor series resistance compensation was used.

Statistics

Means were compared using the unpaired t-test. Multiple comparisons were made using an ANOVA test, followed by a post-hoc Schaffe or Bonfferoni test. Cumulative probabilities of mEPSC parameters were compared using a Kolmogorov-Smirnov test.

Results

Filopodia are formed by microglia during postnatal development

To investigate whether spine structures are formed at regions of microglia contact, I first performed *in vivo* time lapse imaging using two-photon microscopy. Microglia were visualized by using Iba1-EGFP mice expressing EGFP specifically in microglia (Hirasawa et al., 2005). Consistent with previous reports (Hatanaka et al., 2004;Sehara et al., 2010), *in utero* electroporation with pCALNL-DsRed-express or pCALNL-tdTomato performed at E14-15 (see Methods), selectively stained neurons located in L2/3 with RFP (Figure 1A). Hence both microglia (green) and neurons (red) could be simultaneously imaged *in vivo* after making an open cranial windows. To examine the possibility of surgical damage or activation of microglia. I compared microglia morphology in fixed cortex between intact and open-skulled Iba1-EGFP mice (Figure 9). Three parameters are examined; soma size, number of primary processes, and process-ramification area, measured by circumscribing with polygonal object the area covered by processes defined by connecting the outer points of the microglia's ramified arbor. Neither of these three parameters were significantly different between intact and open-skulled mice (Figure 9Bi; intact = $60.2 \pm 3.3 \mu\text{m}^2$, open-skull = $61.6 \pm 2.8 \mu\text{m}^2$,

Bii; intact = $5.0 \pm 0.5 \mu\text{m}^2$, open-skull = $5.3 \pm 0.3 \mu\text{m}^2$, Biii; intact = $1111.4 \pm 135.5 \mu\text{m}^2$, open-skull = $1029.6 \pm 51.8 \mu\text{m}^2$, unpaired t-test).

To investigate whether microglia contribute to synapse formation, we focused on developmental phase when synapse number is rapidly increased. In the rodents neocortex, P8-10 is when this rapid increase begins (Felipe et al., 1997), and also the time when the major ascending projections to the barrel cortex, connecting L4 to L2/3 begins (Bender et al., 2006). During this period, I observed that filopodia-like protrusions were generated at the dendritic site of microglia contacts (Figure 1B). To examine whether microglia contact was indeed associated with generation of these protrusion, I compared the protrusion formation rate between microglia contacted regions and adjacent non-contacted regions (10 μm away from contacted-site). The formation rate at contacted regions was significantly higher than that at non-contacted regions (Figure 1C; adjacent = $5.4 \pm 2.9 \%$, contacted = $46.5 \pm 7.6 \%$; $P < 0.01$; paired t-test). Most (90 %) of the newly formed protrusions induced by microglia contact appeared without a head structure, and were characterized as filopodia ($n = 27$). The other, 10 % of protrusions had a head structure and were considered as, spines structure ($n = 3$). These newly formed filopodia sometimes retracted during the imaging session. However, the survival rate of contacted newly formed protrusions was

similar to those formed without microglia contact (Figure 1D) Therefore, microglia-induced filopodia are not easier to retract than others. Newly formed dendritic filopodia that appeared after or during microglia contact accounted for approximately 8% of all newly generated protrusions (10 of 109 protrusions).

During time lapse imaging at a 5 minutes interval, 57 % of microglia-contacted newly formed filopodia appeared during the same 5 minutes imaging frame as that of the microglia contact (21 of 37 filopodia). Hence, it was possible that microglia preferentially contacted newly generated spines. To distinguish if microglia contact occurred before or after filopodia appearance, I performed real time imaging with a higher temporal resolution (interval was 1.6 sec). This real time imaging revealed that microglia first contacted the dendritic shaft, followed by the generation of filopodia at the contacted dendritic site (Figure 2A). To quantitatively analyze microglia contact and filopodia formation, I plotted the time from microglia contact to filopodia formation. Almost all filopodia formation occurred within 10 minutes after microglia contact (91.7%), and the median value was 3 minutes (Figure 2B). This indicates that microglia contact is prior to filopodia formation, and suggests that microglia contact initiates filopodia formation at P8-10 in somatosensory cortex.

Microglia induced filopodia formation is age dependent

Next I investigated whether microglia-induced filopodia formation was constantly observed throughout development by similarly measuring microglia-dendrite interactions with time lapse imaging at P12-14 and P26-30. At P12-14, the critical period of circuit formation in the barrel cortex (Stern et al., 2001;Shepherd et al., 2003), the formation rate of filopodia was not significantly different between microglia contacted regions and adjacent regions (Figure 3A; adjacent = 6.0 ± 3.2 %, contacted = 14.5 ± 6.6 %). A similar result was seen for interactions in P26-30 mice (Figure 3A; adjacent = 14.6 ± 6.5 %, contacted = 17.3 ± 6.0 %). Thus, microglia-induced filopodia formation is specifically limited to P8-10 aged mice.

TSP1 released from activated microglia may contribute to microglia-induced filopodia formation

Microglia in the immature brain have features resembling activated microglia (Dalmau et al., 2003;Hristova et al., 2010). For example, activated microglia have an amoeboid-shape with a larger soma size and with less processes compared with ramified (resting) microglia (Thored et al., 2009;Wake et al., 2009;Yamada and Jinno, 2013). I examined these morphological characteristics of microglia in immature barrel cortex after brain

fixation. Three parameters were quantified: soma size, number of primary processes, and the area occupied by single microglia. The soma size of P8-10 microglia was bigger than for P12-14 or adult mice (Figure 3Ci; P8-10 = $60.2 \pm 3.3 \mu\text{m}^2$, P12-14 = $42.6 \pm 3.9 \mu\text{m}^2$, P60< = $40.5 \pm 1.9 \mu\text{m}^2$, $P < 0.01$, ANOVA, post hoc: Scheffe). The number of primary processes gradually increased over development (Figure 3Cii; P8-10 = 5.0 ± 0.5 , P12-14 = 6.1 ± 0.5 , P60< = 6.8 ± 0.5 , There were significant differences between P8-10 and P60< ; $P < 0.01$, ANOVA, post hoc: Scheffe). The microglia process area was significantly smaller at P8-10 than that at later stage of development (Figure 3Ciii; P8-10 = $1111.4 \pm 135.5 \mu\text{m}^2$, P12-14 = $1715.1 \pm 128.3 \mu\text{m}^2$, P60< = $2360.1 \pm 159.4 \mu\text{m}^2$, significantly difference between P8-10 and P12-14 at $P < 0.05$, and between P8-10 and P60< at $P < 0.01$, ANOVA, post hoc: Scheffe). These results suggest that microglia have more activated morphology at P8-10, compared with those at adult, and even compared with P12-14.

To examine whether the activation state of microglia is important for microglia-induced filopodia formation, I inhibited microglia activation using minocycline treatment (Lai and Todd, 2006; Schafer et al., 2012). Minocycline was injected intraperitoneal (i.p.; 75 mg/kg) daily between P5 and P11 and filopodia formation examined again at P8-10. The formation rate of filopodia in minocycline injected mice

was significantly decreased compared with that in saline injected control mice (Figure 3D; saline = 51.4 ± 9.9 %, minocycline = 31.4 ± 5.8 %, $P < 0.05$, unpaired t-test).

Hence it appears that the activated-like state of immature microglia is important for filopodia formation. It is known that activated microglia express some molecules involved in synapse formation, such as brain derived neurotrophic factor (BDNF) and TSP1. BDNF is well known to increase the spine number through neuronal tropomyosin receptor kinase b receptor (TrkB) (Ji et al., 2005). Additionally, BDNF increases the filopodia density (Eom et al., 2003) and previous report have suggested that BDNF-TrkB pathway is involved in the filopodia formation (Gomes et al., 2006). TSP1 is also known to be involved in synaptogenesis following release from glial cells (Christopherson et al., 2005). Activated microglia also express TSP1 which can induce neurite outgrowth (Chamak et al., 1994). Thus I examined whether these two molecules are expressed in immature microglia by immunohistochemistry in Iba1-EGFP mice. I could not clearly detect the staining for BDNF in microglia at any age (data not shown). On the other hand at P8, staining of TSP1 was merged with EGFP localization in microglia processes. The area merged with TSP1 staining and EGFP expression became less at P14. In P60, the merged area was scarcely observed (Figure 4A). EGFP is expressed in the intracellular space of microglia in Iba1-EGFP mice.

Given the thickness of one XY image plane is very thin when using confocal microscopy, there is a high possibility that TSP1 is also located within microglia during postnatal development. The high expression of TSP1 within microglia at P8-10 suggested a possible contribution to microglia-induced filopodia formation. Gabapentin (GBP) is a blocker of the TSP receptor, which is $\alpha 2\delta$ -1 subunit of voltage-dependent Ca^{2+} channel (Eroglu et al., 2009). Formation rate of microglia-induced filopodia in GBP injected mice was significantly decreased compared with that in control mice (Figure 4B; Saline = 51.4 ± 9.9 %, GBP = 22.3 ± 7.5 %, $P < 0.05$, unpaired t-test). This result suggests that TSP1 is involved in microglia-induced filopodia formation.

Microglia contact drives actin accumulation in the dendrite

The structural changes involved in filopodia formation requires some cytoskeleton reconstruction, and filopodia are known to be actin rich structures (Korobova and Svitkina, 2010). Hence I attempted to visualize the mobility of actin filaments and how this may change upon the microglia contact. For these experiments, I used cortical slice cultures obtained at P5 from Iba1-EGFP mice (See methods). Microglia in these cultures had a similar activated phenotype, with a large soma and several short processes (Figure 5A). Furthermore, microglia contact onto dendrites of these cultured

neurons was also followed by filopodia formation indicating the same ability of microglia in the cortical slice cultures to form the filopodia. To visualize actin accumulation in the dendrites, neurons were transfected with pCMV-lifeact-mCherry using ballistic transfection method (Riedl et al., 2008; Riedl et al., 2010; Foehring et al., 2011). Red fluorescence was observed throughout the entire transfected neuron. The dendritic spine heads were stained particularly densely because they are actin rich structures, suggesting that this staining could be potentially useful to examine actin mobility in neurons and their processes. Interestingly, sequentially to microglia contact onto the dendrites, actin, observed as mCherry fluorescence, gradually accumulated at the local site within the dendritic shaft on which microglia had made contact. Following this accumulation of actin in the dendritic shaft, was the generation and elongation of filopodia-like structures from this dendritic site. Actin accumulation was gradually enhanced after microglia contact, and reached maximal intensity just before the generation of filopodia. Conversely, dendritic actin was gradually decreased after filopodia formation (Figure 5 B, C). This result suggests that microglia contact induces dendritic actin accumulation that then enables the generation of the filopodia.

Microglia-induced filopodia contributes to functional synapses formation

It was previously reported that filopodia in the developing nervous system made contacts with axons and formed functional synapses (Fiala et al., 1998). The presence of dendritic filopodia coincides with an intense burst of synaptogenesis (Fiala et al., 1998), suggesting that filopodia are the precursors of spines (Ziv and Smith, 1996; Fiala et al., 1998; Lendvai et al., 2000). To examine whether the microglia-induced filopodia eventually became spines, I examined the spine density in the barrel cortex of minocycline-injected mice, because minocycline injection reduces microglia mediated filopodia formation (Figure 3D). Spine density was significantly decreased in minocycline-injected mice compared with saline-injected mice (Figure 6B; saline = 0.7 ± 0.02 , minocycline = 0.6 ± 0.02 , $P < 0.05$, unpaired t-test).

When microglia were ablated by withdrawing Dox from Iba1-tTA::tetO-DTA mice (Stanger et al., 2007; Tanaka et al., 2012), from days P5-11, the spine density was significantly decreased in basal dendrites of L2/3 pyramidal neurons at P11, compared with the control Iba1-tTA mice (Figure 7D; Control = 0.7 ± 0.02 , DTA = 0.4 ± 0.02 , $P < 0.01$, unpaired t-test). Immunohistochemical examination revealed that Dox withdrawal reduce the density of Iba1-positive microglia by approximately 50 % following three days after Dox removal in immature mice (Figure 7B; control =

0.08±0.006 10⁻⁵/μm³, DTA = 0.04±0.005 10⁻⁵/μm³, *P* < 0.01, unpaired t-test). Changing Dox levels may alter the activation state of microglia (Jantzie et al., 2005; Sultan et al., 2013), and hence Iba1-tTA mice were used as controls for these experiments, with Dox removal performed as in Iba1-tTA::tetO-DTA mice. Furthermore, microglia are activated by cell death which triggers microglia to take on phagocytic activity (Koizumi et al., 2007). Thus, microglia activated by dead cells may phagocytose and thereby eliminate synapses. Also, it was recently reported that microglia increase the survival of L5 cortical neurons during development (Ueno et al., 2013). Microglia ablation may therefore affect survival of cortical neurons and decrease the spine number. However, I also confirmed that spine density was decreased by inhibiting microglia by minocycline injection from P5-11 (Figure 6B). Unlike Iba1-tTA::tetO-DTA mice, microglia do not die in these minocycline injected mice (Schafer et al., 2012). Together these results suggest that microglia contributes to an increase in spine density of barrel cortex at P5-11.

Finally, to investigate whether microglia-induced filopodia became functional synapses, I recorded mEPSCs from L2/3 pyramidal neurons in cortical slices from Iba1-tTA::tetO-DTA mice using whole cell patch clamp. Withdrawal of Dox from P5-11 was again achieved by removal from the diet of the mothers. The frequency of mEPSCs was significantly decreased compared with that in control Iba1-tTA mice (Figure 8Bi;

Control = 1.7 ± 0.2 , DTA = 0.8 ± 0.1 , $P < 0.01$, unpaired t-test). In contrast, the amplitude of mEPSCs was not significantly different in the Iba1-tTA::tetO-DTA mice (Figure 8Ci; Control = 11.7 ± 0.5 , DTA = 12.9 ± 0.7 , unpaired t-test). Hence partial ablation of microglia reduces the number of functional synapses, presumably by reducing filopodia formation and spine density.

Discussion

Microglia functions for neurons

Microglia have well known roles in activation by traumatic injury or infections and subsequent phagocytosis of neuronal debris (Graeber and Streit, 2010; Perry et al., 2010). Recent studies have revealed additional and more direct and possibly dynamic interactions between microglia and neuronal elements. These include making physical contacts such as neurite in cultured neurons (Linnartz et al., 2012), or axonal terminals and synapses projecting on to injured and degenerating neurons (Oliveira et al., 2004; Yamada et al., 2008). In these cases, microglia process move into the synaptic cleft, result in a removal of the afferent inputs onto the axotomized motoneurons (Blinzinger and Kreutzberg, 1968; Graeber and Streit, 2010). Such synaptic stripping is also observed in rat cerebral cortex following microglia activation induced by an injection of bacterial fragments (Trapp et al., 2007). In the ischemic cortex, prolonged microglia-synapse contacts were observed by two-photon imaging *in vivo* and occasionally lead to an elimination of the contacted synapses (Brown et al., 2007; Wake et al., 2009). However microglia-neuron interactions are also becoming evident in normal, uninjured brain. *In vivo* two-photon microscopy revealed that microglia

processes regularly contacted pre- and post-synaptic structures in intact mouse cortex (Wake et al., 2009). In particular, microglia-neuron contacts have been suggested to be important for neuronal circuit refinement during development. The synaptic pruning that accompanies developmental refinements of neural circuits coincides with a period of increased density of resident CNS microglia and involves microglia phagocytosis of synapses (Tremblay et al., 2010; Schafer et al., 2012). However the focus of the role of microglia has been on the process of synapse elimination. Additional reports from developmental mice have also revealed that microglia affected the numbers and/or survival of cortical neurons (Cunningham et al., 2013; Ueno et al., 2013) and the maturity of, synapses in somatosensory cortex (Hoshiko et al., 2012). However, none of these reports consider or demonstrate that microglia play a role in synapse formation, as shown here.

Very recently, an indirect *in vitro* study hinted at a possible contribution of microglia to synapse formation, by incubation of estradiol in co-cultured preoptic neurons and microglia (Lenz et al., 2013). In the preoptic area, which is the region necessary for the expression of the adult male sex behavior, the major morphological sex differences are organized by the perinatal actions of estradiol (Simerly, 2002). At this period, microglia in male mice have more activated state than that in female mice. Microglia in female

mice are also activated by estradiol treatment, and they showed that estradiol application to co-cultures of preoptic neurons and microglia from female pups increased the number of spine-like structures. This effect was not observed in pure neuronal cultures, implicating activated microglia and estradiol in some way to be involved in the formation of spine-like structure. However the precise mechanisms are unanswered. The present study directly demonstrates both *in vitro* and *in vivo* that microglia contact onto dendrites induces filopodia formation in immature somatosensory cortex (Figure 1, 2). Microglia inhibition, by partial ablation and by pharmacological inhibition decreased the density of synapses in the pyramidal neurons (Figure 6, 7, 8). Thus, my experiments add to the reported functions of microglia, suggesting they have the ability to generate synapses in developing brain. This strongly contrasts with their role in synapse elimination.

Activated-like phenotype of microglia is important for filopodia formation

As reported, microglia contribute to synapse elimination in developing visual cortex of mice at P28-32 (Tremblay et al., 2010). At this developmental stage, microglia have already changed to a more ramified “resting” and adult-like morphology. In contrast, microglia in the present study at P5-11 showed morphological characteristics similar to

the activated morphology (Figure 3B, C). After migrating to the CNS during embryogenesis and in the first few postnatal days. Microglia have an activated-like morphology, gradually changing over postnatal development to the resting (more ramified), adult CNS resident microglia phenotype. My present results showed that the ability of microglia-dendrite contact to form filopodia is restricted to a very limited period in development, at P8-10 or earlier (Figure 3A). Thus, whether microglia-neuron interaction causes synapse formation or synapse elimination may be defined by their phenotype, which changes over development. However, microglia at P5-8 (with the presumed activated like phenotype) are able to eliminate synapses in the lateral geniculate nucleus (LGN) (Schafer et al., 2012). This age corresponds to a critical period when eye-specific segregation of inputs from retinal ganglion cells to LGN cells takes place (Schafer et al., 2012). In the visual cortex, synapse elimination by microglia also takes place during the critical period (Tremblay et al., 2010). Although synapse elimination by microglia in visual cortex and LGN occurs at different ages, it is matched to the specific time when these neural circuits are being refined (Penn et al., 1998; Hooks and Chen, 2006). In the present study, the time period of microglia-induced filopodia formation (P8-10) corresponds with the developmental period when massive formation of excitatory synapses takes place in the barrel cortex (Felipe et al., 1997).

Specifically, the formation of functional synapses from L4 excitatory neurons to L2/3 pyramidal neurons begins at this developmental period (Bender et al., 2003; Bender et al., 2006). Hence whether microglia-neuron contact is involved in synapse elimination or formation may depend not directly on age but on the specific stage of neural development, either the period of filopodia formation and synapse growth, or the period of synapse elimination and circuit refinement.

Molecular mechanisms of microglia-induced filopodia formation

A range of pre- and post-synaptic molecules are thought to work in concert to build a CNS synapse. One of these important molecules is the neuronal adhesion proteins that constitute an important part of the intrinsic synaptic machinery (Dalva et al., 2007).

For example, EphB, which is located on the surface of dendritic filopodia and bind to presynaptic ephrin-B, changes filopodia motility and is a key step leading to formation of synapse (Kayser et al., 2008). Additional soluble neuronal factors also contribute to this synaptogenesis. BDNF has been shown to contribute to an increase in spine and synapse number, and different forms of neuronal circuit plasticity (Tyler and Pozzo-Miller, 2003; Hensch, 2005; Ji et al., 2010). Expression of BDNF in microglia is enhanced spinal cord of chronic pain, resulting in an establishment of pathological

functional circuits (Coull et al., 2005). However, I could not find a distinct expression of BDNF in microglia in mice barrel cortex at P8 (not shown), at which age a massive increase in synapses is apparent in this cortical region (Felipe et al., 1997). Another more recent soluble secreted factor implicated in synapse formation is the TSPs. TSPs secreted from astrocyte induces synaptogenesis in developing mouse cortex (Christopherson et al., 2005; Eroglu et al., 2009). Interestingly, both BDNF (Nakajima et al., 2001) and TSPs (Chamak et al., 1994) are expressed in cultured microglia. Activated microglia that express TSP1, can induce neurite outgrowth (Chamak et al., 1994). TSP receptor, the $\alpha 2\delta$ -1 subunit of the voltage-dependent Ca^{2+} channel complex, is expressed in the cortex (Cole et al., 2005) and co-localizes at synapses in immature mice (Eroglu et al., 2009). Consistently, I also detected TSP1 in microglia processes in the barrel cortex at P8 (Figure 4A), and gabapentin (GBP), a blocker of the TSP receptor, significantly reduced microglia induced filopodia formation (Figure 4B). In addition, TSP1 binds to neuroligin1, results in an increase in the number of synapses in cultured hippocampal neurons (Xu et al., 2010). TSP1 can also bind to $\alpha 3\beta 1$ -integrin protein which also results in neurite outgrowth (DeFreitas et al., 1995). I propose that TSP1 can be released from microglia and promotes filopodia formation in developing cortex.

However, given that filopodia formed at the precise dendritic sites on which microglia had made contact (Figure 2A), it is likely that some more specific contact-induced signal also exists. Adhesion molecules are a possible molecular mechanism involved in contact induced signals. For example, integrin is highly expressed in activated microglia (Hailer et al., 1997; Kloss et al., 2001) and $\alpha 4$, $\alpha 5$, $\alpha 6$, αX , $\beta 2$ integrins are highly expressed at this approximate developmental stage in mouse brain, gradually decreasing with further development (Hristova et al., 2010). Specifically the $\alpha L\beta 2$ integrin (lymphocyte function associated antigen 1 (LFA-1)) is expressed only in microglia in the CNS, and binds to the intercellular adhesion molecule-5 (ICAM-5, telencephalin) (Mizuno et al., 1999). ICAM-5 is known to bind to integrin and regulate synapse formation (Ning et al., 2013). ICAM-5 could also be potentially involved in filopodia formation through actions on the actin adaptor protein, ERM (ezrin/radixin/moesin) family proteins (Furutani et al., 2007). Future experiments should evaluate the contribution of these adhesion molecules to microglia-induced filopodia formation as well as soluble signals.

In conclusion, I have directly demonstrated for the first time that microglia contribute to excitatory synapse formation through filopodia formation in L2/3

pyramidal neurons in the developing mice neocortex. Microglia are known to be important for neuronal circuit development via synapse elimination and now it we show that microglia are also involved in synapse formation. Synaptogenesis and synaptogenesis is important to make appropriate cortical networks, and hence microglia are important for this neuronal circuit development. Recent reports have implicated microglia as the primary site of defects in Rett's syndrome, and Hoxb8-deficiency, a model of obsessive compulsive disorder (Chen et al., 2010;Derecki et al., 2012), and some mice models of other developmental disorders show abnormal spine structure and density (Cruz-Martin et al., 2010;Landi et al., 2011). Thus my data offer insight into the role of microglia in generate functional synapses in the developing CNS, which expands the list of functions attributed to microglia in health and diseased brain, potentially providing important mechanistic insight into diseased CNS.

Acknowledgements

I would like to thank Professor Junichi Nabekura for the mentorship of this thesis. I also thank to Dr. Kei Eto, he gave me a lot of advices and suggestions, and Tastuko Ooba, she gave me a lots of help for mice handling and assistance of experiments. I appreciate to Professor Schuichi Koizumi and Assistant professor Keisuke Shibata at Yamanashi University for TSP1 immunohistochemistry experiment. I also appreciate to Associate professor Hideji Murakoshi at Supportive Center for Brain Research of National Institute for Physiological Sciences for actin visualization. I also thank to Professor Kenji F Tanaka at Keio University for providing Iba1-tTA mice. I thank Spectrography and Bioimaging Facility, NIBB Core Research Facilities for technical support.

I am also indebted all members of Laboratory of Homeostatic Development and National Institute for Physiological Sciences for their supports and inspiring discussion.

References

- Bender, K.J., Allen, C.B., Bender, V.A., and Feldman, D.E. (2006). Synaptic basis for whisker deprivation-induced synaptic depression in rat somatosensory cortex. *J Neurosci* 26, 4155-4165.
- Bender, K.J., Rangel, J., and Feldman, D.E. (2003). Development of Columnar Topography in the Excitatory Layer 4 to Layer 2/3 Projection in Rat Barrel Cortex. *J Neurosci* 23, 8759-8770.
- Blinzinger, K., and Kreutzberg, G. (1968). Displacement of synaptic terminals from regenerating motoneurons by microglia cells. *Z Zellforsch Mikrosk Anat* 85, 145-157.
- Brown, C.E., Li, P., Boyd, J.D., Delaney, K.R., and Murphy, T.H. (2007). Extensive Turnover of Dendritic Spines and Vascular Remodeling in Cortical Tissues Recovering from Stroke. *J Neurosci* 27, 4101-4109.
- Chamak, B., Morandi, V., and Mallat, M. (1994). Brain Macrophages Stimulate Neurite Growth and Regeneration by Secreting Thrombospondin. *J Neurosci Res* 38, 221-233.
- Chen, S.K., Tvrdik, P., Peden, E., Cho, S., Wu, S., Spangrude, G., and Capecchi, M.R. (2010). Hematopoietic origin of pathological grooming in Hoxb8 mutant mice. *Cell* 141, 775-785.
- Christopherson, K.S., Ullian, E.M., Stokes, C.C., Mallowney, C.E., Hell, J.W., Agah, A., Lawler, J., Mosher, D.F., Bornstein, P., and Barres, B.A. (2005). Thrombospondins are astrocyte-secreted proteins that promote CNS synaptogenesis. *Cell* 120, 421-433.
- Cole, R.L., Lechner, S.M., Williams, M.E., Prodanovich, P., Bleicher, L., Varney, M.A., and Gu, G. (2005). Differential distribution of voltage-gated calcium channel alpha-2 delta (alpha2delta) subunit mRNA-containing cells in the rat central nervous system and the dorsal root ganglia. *J Comp Neurol* 491, 246-269.
- Coull, J.A., Beggs, S., Boudreau, D., Boivin, D., Tsuda, M., Inoue, K., Gravel, C., Salter, M.W., and De Koninck, Y. (2005). BDNF from microglia causes the shift in neuronal anion gradient underlying neuropathic pain. *Nature* 438, 1017-1021.
- Cruz-Martin, A., Crespo, M., and Portera-Cailliau, C. (2010). Delayed stabilization of dendritic spines in fragile X mice. *J Neurosci* 30, 7793-7803.

- Cunningham, C.L., Martinez-Cerdeno, V., and Noctor, S.C. (2013). Microglia regulate the number of neural precursor cells in the developing cerebral cortex. *J Neurosci* 33, 4216-4233.
- Dalmau, I., Vela, J.M., Gonzalez, B., Finsen, B., and Castellano, B. (2003). Dynamics of microglia in the developing rat brain. *J Comp Neurol* 458, 144-157.
- Dalva, M.B., McClelland, A.C., and Kayser, M.S. (2007). Cell adhesion molecules: signalling functions at the synapse. *Nat Rev Neurosci* 8, 206-220.
- Defreitas, M.F., Yoshida, C.K., Frezler, W.A., Mendrick, D.L., Kypka, R.M., and Reichardt, L.F. (1995). Identification of Integrin alpha3beta1 as a Neuronal Thrombospondin Receptor Mediating Neurite Outgrowth. *Neuron* 15, 333-343.
- Derecki, N.C., Cronk, J.C., Lu, Z., Xu, E., Abbott, S.B., Guyenet, P.G., and Kipnis, J. (2012). Wild-type microglia arrest pathology in a mouse model of Rett syndrome. *Nature* 484, 105-109.
- Elston, G.N., Oga, T., and Fujita, I. (2009). Spinogenesis and pruning scales across functional hierarchies. *J Neurosci* 29, 3271-3275.
- Eom, T., Antar, L., Singer, R., and Bassell, G. (2003). Localization of a beta-Actin Messenger Ribonucleoprotein Complex with Zipcode-Binding Protein Modulates the Density of Dendritic Filopodia and Filopodial Synapses. *J Neurosci* 23, 10433-10444
- Eroglu, C., Allen, N.J., Susman, M.W., O'Rourke, N.A., Park, C.Y., Ozkan, E., Chakraborty, C., Mulinyawe, S.B., Annis, D.S., Huberman, A.D., Green, E.M., Lawler, J., Dolmetsch, R., Garcia, K.C., Smith, S.J., Luo, Z.D., Rosenthal, A., Mosher, D.F., and Barres, B.A. (2009). Gabapentin receptor alpha2delta-1 is a neuronal thrombospondin receptor responsible for excitatory CNS synaptogenesis. *Cell* 139, 380-392.
- Felipe, J.D., Marco, P., Fairén, A., and Jones, E.G. (1997). Inhibitory Synaptogenesis in Mouse Somatosensory Cortex. *Cerebral Cortex* 7, 619-634.
- Fiala, J.C., Feinberg, M., Popov, V., and Harris, K.M. (1998). Synaptogenesis Via Dendritic Filopodia in Developing Hippocampal Area CA1. *J Neurosci* 18, 8900-8911.
- Foehring, R.C., Guan, D., Toleman, T., and Cantrell, A.R. (2011). Whole cell recording from

- an organotypic slice preparation of neocortex. *J Vis Exp* 52, e2600.
- Furutani, Y., Matsuno, H., Kawasaki, M., Sasaki, T., Mori, K., and Yoshihara, Y. (2007). Interaction between telencephalin and ERM family proteins mediates dendritic filopodia formation. *J Neurosci* 27, 8866-8876.
- Gomes, R.A., Hampton, C., El-Sabeawy, F., Sabo, S.L., and Mcallister, A.K. (2006). The dynamic distribution of TrkB receptors before, during, and after synapse formation between cortical neurons. *J Neurosci* 26, 11487-11500.
- Graeber, M.B., and Streit, W.J. (2010). Microglia: biology and pathology. *Acta Neuropathologica* 119, 89-105.
- Hailer, N.P., Bechmann, I., Heizmann, S., and Nitsch, R. (1997). Adhesion Molecule Expression on Phagocytic Microglia Cells Following Anterograde Degeneration of Perforant Path Axons. *Hippocampus* 7, 341-349.
- Hatanaka, Y., Hisanaga, S., Heizmann, C.W., and Murakami, F. (2004). Distinct migratory behavior of early- and late-born neurons derived from the cortical ventricular zone. *J Comp Neurol* 479, 1-14.
- Hensch, T.K. (2005). Critical period plasticity in local cortical circuits. *Nat Rev Neurosci* 6, 877-888.
- Hirasawa, T., Ohsawa, K., Imai, Y., Ondo, Y., Akazawa, C., Uchino, S., and Kohsaka, S. (2005). Visualization of microglia in living tissues using Iba1-EGFP transgenic mice. *J Neurosci Res* 81, 357-362.
- Hooks, B.M., and Chen, C. (2006). Distinct roles for spontaneous and visual activity in remodeling of the retinogeniculate synapse. *Neuron* 52, 281-291.
- Hoshiko, M., Arnoux, I., Avignone, E., Yamamoto, N., and Audinat, E. (2012). Deficiency of the microglia receptor CX3CR1 impairs postnatal functional development of thalamocortical synapses in the barrel cortex. *J Neurosci* 32, 15106-15111.
- Hristova, M., Cuthill, D., Zbarsky, V., Acosta-Saltos, A., Wallace, A., Blight, K., Buckley, S.M., Peebles, D., Heuer, H., Waddington, S.N., and Raivich, G. (2010). Activation and deactivation of periventricular white matter phagocytes during postnatal mouse development. *Glia* 58, 11-28.
- Jantzie, L.L., Cheung, P.Y., and Todd, K.G. (2005). Doxycycline reduces cleaved caspase-3 and

- microglia activation in an animal model of neonatal hypoxia-ischemia. *J Cereb Blood Flow Metab* 25, 314-324.
- Ji, Y., Lu, Y., Yang, F., Shen, W., Tang, T.T., Feng, L., Duan, S., and Lu, B. (2010). Acute and gradual increases in BDNF concentration elicit distinct signaling and functions in neurons. *Nat Neurosci* 13, 302-309.
- Ji, Y., Pang, P.T., Feng, L., and Lu, B. (2005). Cyclic AMP controls BDNF-induced TrkB phosphorylation and dendritic spine formation in mature hippocampal neurons. *Nat Neurosci* 8, 164-172.
- Kayser, M.S., Nolt, M.J., and Dalva, M.B. (2008). EphB receptors couple dendritic filopodia motility to synapse formation. *Neuron* 59, 56-69.
- Kloss, C.U., Bohatschek, M., Kreutzberg, G.W., and Raivich, G. (2001). Effect of lipopolysaccharide on the morphology and integrin immunoreactivity of ramified microglia in the mouse brain and in cell culture. *Exp Neurol* 168, 32-46.
- Koizumi, S., Shigemoto-Mogami, Y., Nasu-Tada, K., Shinozaki, Y., Ohsawa, K., Tsuda, M., Joshi, B.V., Jacobson, K.A., Kohsaka, S., and Inoue, K. (2007). UDP acting at P2Y6 receptors is a mediator of microglia phagocytosis. *Nature* 446, 1091-1095.
- Korobova, F., and Svitkina, T. (2010). Molecular architecture of synaptic actin cytoskeleton in hippocampal neurons reveals a mechanism of dendritic spine morphogenesis. *Mol Biol Cell* 21, 165-176.
- Lai, A.Y., and Todd, K.G. (2006). Hypoxia-activated microglia mediators of neuronal survival are differentially regulated by tetracyclines. *Glia* 53, 809-816.
- Landi, S., Putignano, E., Boggio, E.M., Giustetto, M., Pizzorusso, T., and Ratto, G.M. (2011). The short-time structural plasticity of dendritic spines is altered in a model of Rett syndrome. *Sci Rep* 1, 45.
- Lendvai, B., Stern, E.A., Chen, B., and Svoboda, K. (2000). Experience-dependent plasticity of dendritic spines in the developing rat barrel cortex in vivo. *Nature* 404, 876-881.
- Lenz, K.M., Nugent, B.M., Haliyur, R., and McCarthy, M.M. (2013). Microglia are essential to masculinization of brain and behavior. *J Neurosci* 33, 2761-2772.
- Linnartz, B., Kopatz, J., Tenner, A.J., and Neumann, H. (2012). Sialic acid on the neuronal glycolyx prevents complement C1 binding and complement receptor-3-mediated

- removal by microglia. *J Neurosci* 32, 946-952.
- Mizuno, T., Yoshihara, Y., Kagamiyama, H., Ohsawa, K., Imai, Y., Kohsaka, S., and Mori, K. (1999). Neuronal adhesion molecule telencephalin induces rapid cell spreading of microglia. *Brain Research* 849, 58–66.
- Nakajima, K., Honda, S., Tohyama, Y., Imai, Y., Kohsaka, S., and Kurihara, T. (2001). Neurotrophin Secretion From Cultured Microglia. *Journal of Neuroscience Research* 65, 322–331.
- Nimmerjahn, A., Kirchhoff, F., and Helmchen, F. (2005). Resting microglia cells are highly dynamic surveillants of brain parenchyma in vivo. *Science* 308, 1314-1318.
- Ning, L., Tian, L., Smirnov, S., Vihinen, H., Llano, O., Vick, K., Davis, R.L., Rivera, C., and Gahmberg, C.G. (2013). Interactions between ICAM-5 and beta1 integrins regulate neuronal synapse formation. *J Cell Sci* 126, 77-89.
- Oliveira, A.L.R., Thams, S., Lidman, O., Piehl, F., Kfelt, T.H., Rre, K.K., Lindå, H., and Cullheim, S. (2004). A role for MHC class 1 molecules in synaptic plasticity and regeneration of neurons after axotomy. *Proc Natl Acad Sci USA* 101, 17843-17848.
- Paolicelli, R.C., Bolasco, G., Pagani, F., Maggi, L., Scianni, M., Panzanelli, P., Giustetto, M., Ferreira, T.A., Guiducci, E., Dumas, L., Ragozzino, D., and Gross, C.T. (2011). Synaptic Pruning by Microglia Is Necessary for Normal Brain Development. *Science* 333, 1456-1458.
- Parnass, Z., Tashiro, A., and Yuste, R. (2000). Analysis of Spine Morphological Plasticity in Developing Hippocampal Pyramidal Neurons. *Hippocampus* 10, 561-568.
- Penn, A.A., Riquelme, P.A., Feller, M.B., and Shatz, C.J. (1998). Competition in Retinogeniculate Patterning Driven by Spontaneous Activity. *Science* 279, 2108-2112.
- Perry, V.H., Nicoll, J.a.R., and Holmes, C. (2010). Microglia in neurodegenerative disease. *Nat Rev Neurology* 6, 193-201.
- Riedl, J., Crevenna, A.H., Kessenbrock, K., Yu, J.H., Neukirchen, D., Bista, M., Bradke, F., Jenne, D., Holak, T.A., Werb, Z., Sixt, M., and Wedlich-Soldner, R. (2008). Lifeact: a versatile marker to visualize F-actin. *Nat Methods* 5, 605 - 607.
- Riedl, J., Flynn, K.C., Raducanu, A., Gartner, F., Beck, G., Bosl, M., Bradke, F., Massberg, S., Aszodi, A., Sixt, M., and Wedlich-Soldner, R. (2010). Lifeact mice for studying F-actin

- dynamics. *Nat Methods* 7, 168-169.
- Schafer, D.P., Lehrman, E.K., Kautzman, A.G., Koyama, R., Mardinly, A.R., Yamasaki, R., Ransohoff, R.M., Greenberg, M.E., Barres, B.A., and Stevens, B. (2012). Microglia sculpt postnatal neural circuits in an activity and complement-dependent manner. *Neuron* 74, 691-705.
- Sehara, K., Toda, T., Iwai, L., Wakimoto, M., Tanno, K., Matsubayashi, Y., and Kawasaki, H. (2010). Whisker-related axonal patterns and plasticity of layer 2/3 neurons in the mouse barrel cortex. *J Neurosci* 30, 3082-3092.
- Shepherd, G.M.G., Pologruto, T.A., and Svoboda, K. (2003). Circuit Analysis of Experience-Dependent Plasticity in the Developing Rat Barrel Cortex. *Neuron* 38, 277-289.
- Simerly, R.B. (2002). Wired for reproduction: organization and development of sexually dimorphic circuits in the mammalian forebrain. *Annu Rev Neurosci* 25, 507-536.
- Stanger, B.Z., Tanaka, A.J., and Melton, D.A. (2007). Organ size is limited by the number of embryonic progenitor cells in the pancreas but not the liver. *Nature* 445, 886-891.
- Stern, E.A., Maravall, M., and Svoboda, K. (2001). Rapid Development and Plasticity of Layer 2/3 Maps in Rat Barrel Cortex In Vivo. *Neuron* 31, 305-315.
- Sultan, S., Gebara, E., and Toni, N. (2013). Doxycycline increases neurogenesis and reduces microglia in the adult hippocampus. *Front Neurosci* 7, 131.
- Tanaka, K.F., Matsui, K., Sasaki, T., Sano, H., Sugio, S., Fan, K., Hen, R., Nakai, J., Yanagawa, Y., Hasuwa, H., Okabe, M., Deisseroth, K., Ikenaka, K., and Yamanaka, A. (2012). Expanding the repertoire of optogenetically targeted cells with an enhanced gene expression system. *Cell Rep* 2, 397-406.
- Thored, P., Heldmann, U., Gomes-Leal, W., Gisler, R., Darsalia, V., Taneera, J., Nygren, J.M., Jacobsen, S.E., Ekdahl, C.T., Kokaia, Z., and Lindvall, O. (2009). Long-term accumulation of microglia with proneurogenic phenotype concomitant with persistent neurogenesis in adult subventricular zone after stroke. *Glia* 57, 835-849.
- Trapp, B.D., Wujek, J.R., Criste, G.A., Jalabi, W., Yin, X., Kidd, G.J., Stohlman, S., and Ransohoff, R. (2007). Evidence for synaptic stripping by cortical microglia. *Glia* 55, 360-368.
- Tremblay, M.E., Lowery, R.L., and Majewska, A.K. (2010). Microglia interactions with

- synapses are modulated by visual experience. *PLoS Biol* 8, e1000527.
- Tyler, W.J., and Pozzo-Miller, L. (2003). Miniature synaptic transmission and BDNF modulate dendritic spine growth and form in rat CA1 neurones. *J Physiol* 553, 497-509.
- Ueno, M., Fujita, Y., Tanaka, T., Nakamura, Y., Kikuta, J., Ishii, M., and Yamashita, T. (2013). Layer V cortical neurons require microglia support for survival during postnatal development. *Nat Neurosci* 16, 543-551.
- Wake, H., Moorhouse, A.J., Jinno, S., Kohsaka, S., and Nabekura, J. (2009). Resting microglia directly monitor the functional state of synapses in vivo and determine the fate of ischemic terminals. *J Neurosci* 29, 3974-3980.
- Xu, J., Xiao, N., and Xia, J. (2010). Thrombospondin 1 accelerates synaptogenesis in hippocampal neurons through neuroligin 1. *Nat Neurosci* 13, 22-24.
- Yamada, J., Hayashi, Y., Jinno, S., Wu, Z., Inoue, K., Kohsaka, S., and Nakanishi, H. (2008). Reduced synaptic activity precedes synaptic stripping in vagal motoneurons after axotomy. *Glia* 56, 1448-1462.
- Yamada, J., and Jinno, S. (2013). Novel objective classification of reactive microglia following hypoglossal axotomy using hierarchical cluster analysis. *J Comp Neurol* 521, 1184-1201.
- Ziv, N.E., and Smith, S.J. (1996). Evidence for a Role of Dendritic Filopodia in Synaptogenesis and Spine Formation. *Neuron* 17, 91-102.

Figures

Figure 1. Microglia contact initiates dendritic filopodia formation.

- A. Schematic diagram of pregnant mouse illustrating, *in utero* electroporation was performed of E14 or E15 Iba1-EGFP mice embryos. pCALNL-DsRed-express or pCALNL-tdTomato plasmids were used to label and visualize L2/3 pyramidal neurons, enabling concurrent imaging of microglia (green) and neurons (red).
- B. *In vivo* time-lapse imaging of microglia (green) and neuron (red) interactions in mouse barrel cortex. The set of right side panels show a magnified image of the microglia-neuronal dendrite interaction region shown in the left hand panel. The upper set show both microglia and dendrite, the lower panels shows only the dendrite image. Microglia process contacted a dendrite at designated time zero (yellow arrowhead). A filopodia like protrusion formed at the site of the microglia contact region (5 min, yellow arrowhead). Scale bar 5 μm .
- C. The averaged filopodia formation rate was significantly greater for dendritic regions contacted by microglia as compared to 10 μm adjacent non-contacted region. *** $p < 0.01$, paired t-test (animal $n = 9$, dendrite $n = 21$, Error bar: SE)
- D. The distribution of durations that newly formed filopodia remained in dendrites (survival rate) were not different those forming at regions of microglia contact ($n =$

18) and others that formed at regions without contact ($n = 121$). Error bar: SE.

Figure 1

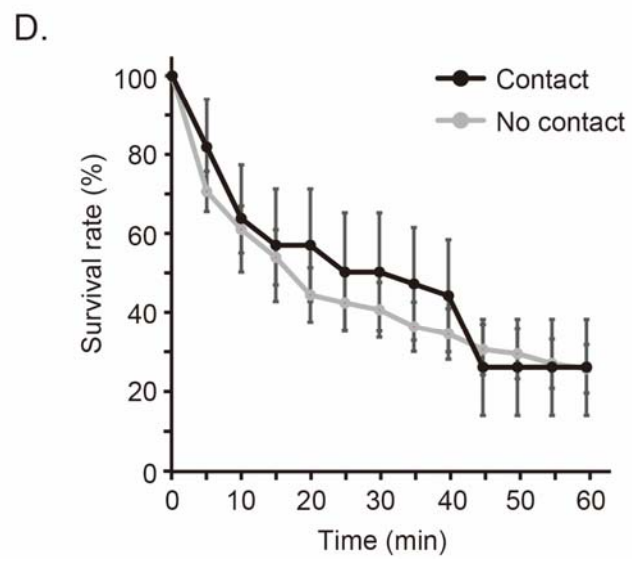
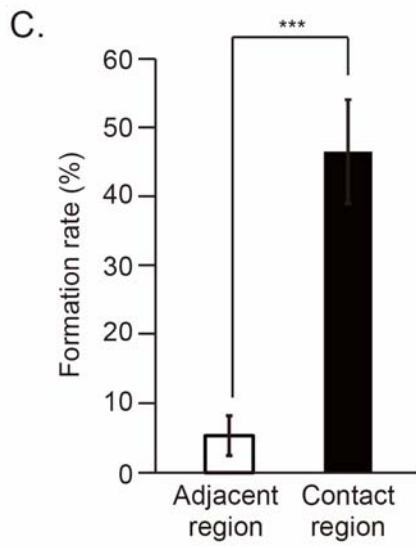
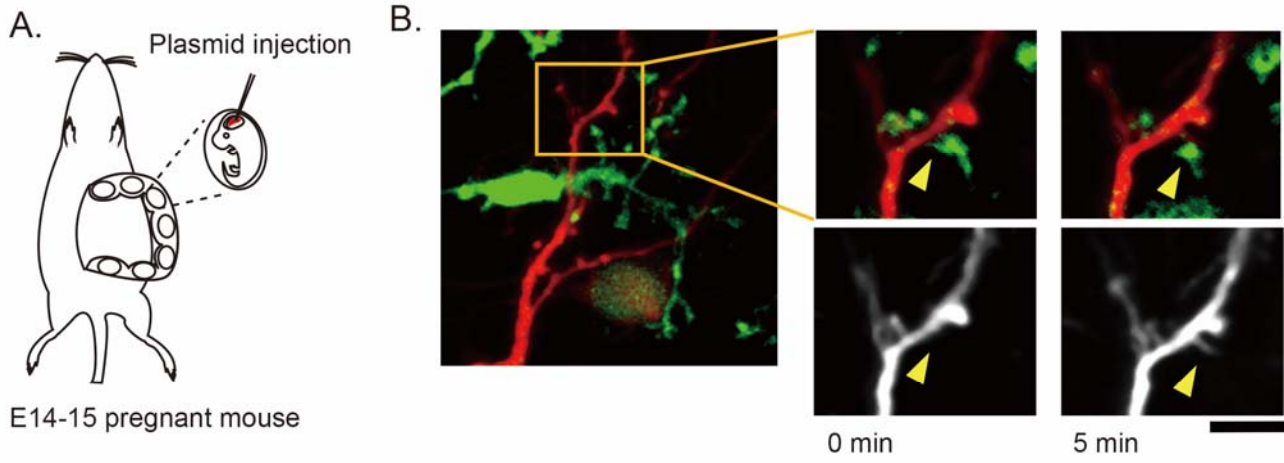
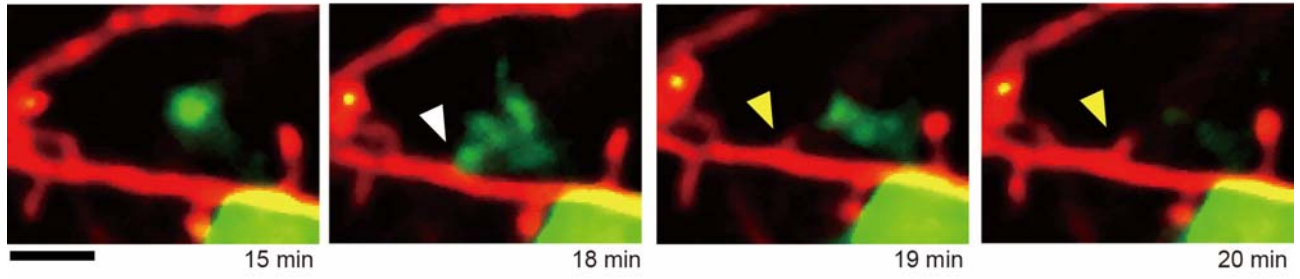


Figure 2. *In vivo* real time imaging of microglia-dendrite contacts and filopodia formation.

- A. A series of 4 time-lapse images (at time from start of imaging as indicated), showing microglia (green) approaching, briefly contacting (white arrowhead) and then withdrawing from a dendrite (red). A dendritic filopodia was formed about 1 minute after the microglia contact (yellow arrowhead).
- B. Distribution of times between from the onset of microglia-dendrite contact and the onset of filopodia formation. The median latency between contact and filopodia formation was 3 minutes. (protrusion n = 12)

Figure 2

A.



B.

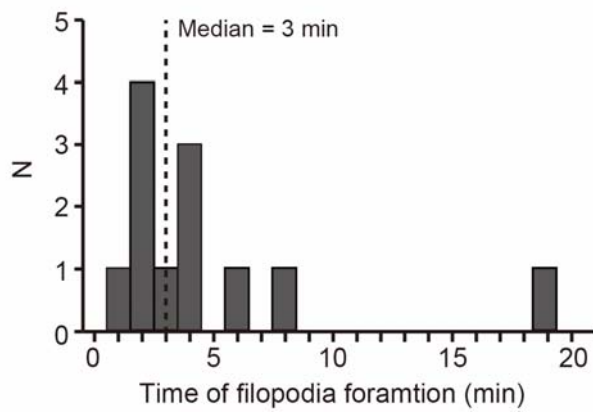


Figure 3. Developmental change in microglia morphology and function

- A. Mean filopodia formation rates following microglia contact with dendrites (black columns) as compared to formation rates of filopodia appearing in non-contacted dendritic regions adjacent to contacted sites (open columns). Compared to P8-10, the formation rate of contacted dendritic regions was reduced to almost the same level as the control adjacent region at P12-14 and P26-30 mice. *** $P < 0.01$ paired t-test (adjacent *vs* contact), + $P < 0.05$ ANOVA, post hoc: Bonferroni (*vs* age), (P8-10:dendrite n=21, P12-14: dendrite n=10, P26-30: dendrite n=12, Error bar: SE)
- B. Developmental change in microglia morphology. Representative images of microglia from fixed Iba1-EGFP mice cortex at P8-10 (left), P12-14 (center) and P60 (right). P8-10 microglia have an amoeboid shape with less processes, indicative of their more activated morphology, compare to P60< mice. Scale bar 20 μm .
- C. Quantification of parameters of microglia morphology at P8-10, P12-14 and above P60. P8-10 microglia have significantly larger cell soma (left panel, C i), but reduced number of primary processes (center panel, C ii) and reduced total process area (right panel, C iii) as compared to older mice. *** $P < 0.01$, * $P < 0.05$, ANOVA, post hoc: Scheffe (P8-10: cell n=14, P12-14 cell n=12, P60< cell n=21, Error bar: SE)
- D. Formation rate of dendritic filopodia at microglia-contacted regions in saline (open

columns) and minocycline (closed columns) i.p. injected mice. Daily minocycline treatment between P5 to imaging day significantly decreased formation rate measured at P8-10 mice. $*p < 0.05$, unpaired t-test (Saline: animal n = 10, dendrite n = 11, Mino: animal n = 9, dendrite n = 12, Error bar: SE)

Figure 3

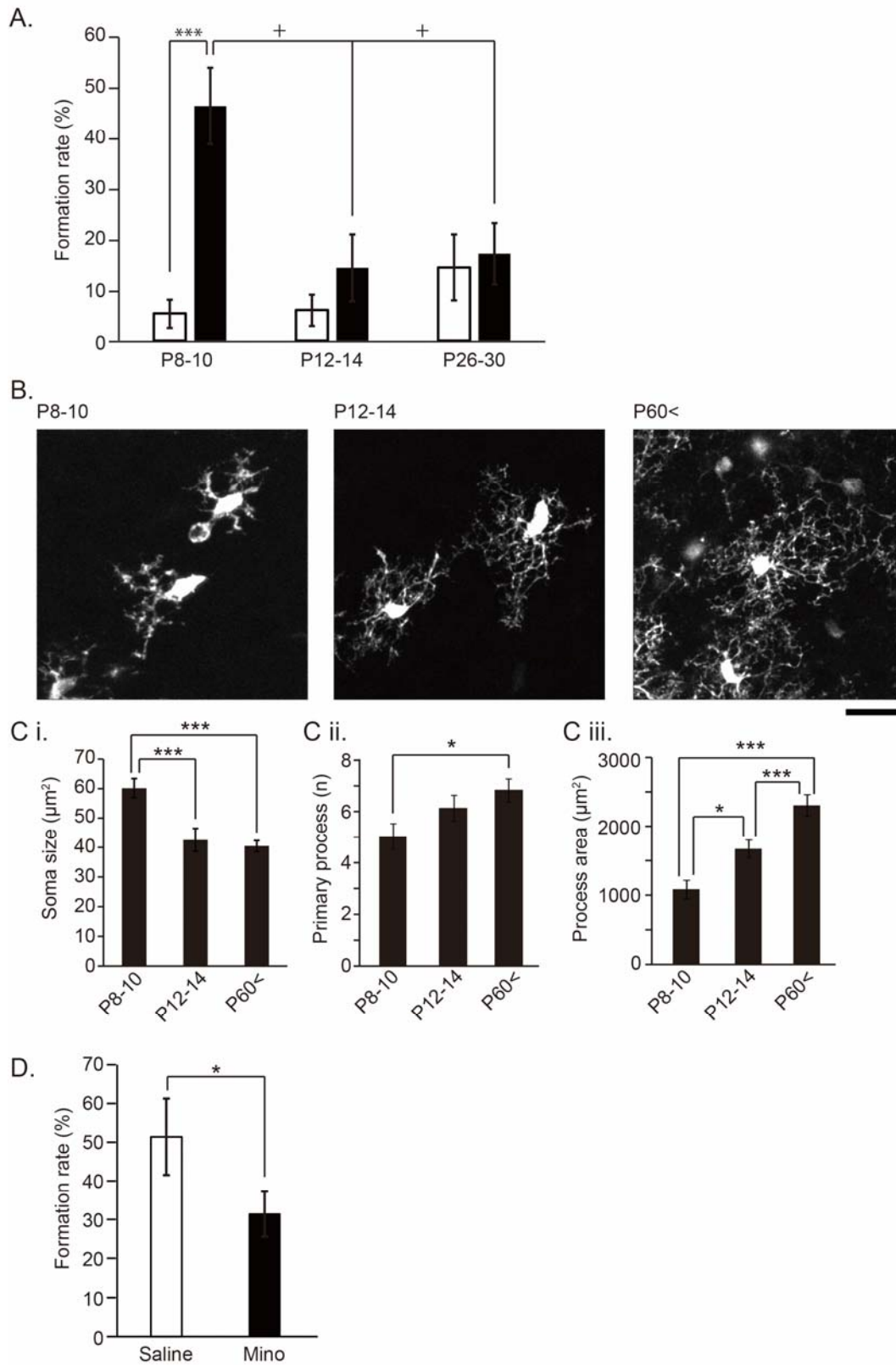


Figure 4. TSP1 is expressed in P8 microglia processes.

- A. Immunohistochemical analysis of TSP1 expression (red) and its colocalization with Iba1 (green) in microglia processes (green) in L2/3 of the somatosensory cortex of P8, P14, and P60 Iba1-EGFP mice. Arrowheads indicate TSP1 expressing microglia processes.
- B. The averaged filopodia formation rate at microglia contacted regions in saline (open columns) and gabapentin (GBP, closed columns) treated mice. Daily injection of GBP in P5 to imaging day significantly decreased filopodia formation, in P8-10 mice presumably by blocking TSP1 signalling at its receptor. * $p < 0.05$, unpaired t-test (Saline: animal n = 10, dendrite n = 11, GBP: animal n = 3, dendrite n = 7, Error bar: SE)

Figure 4

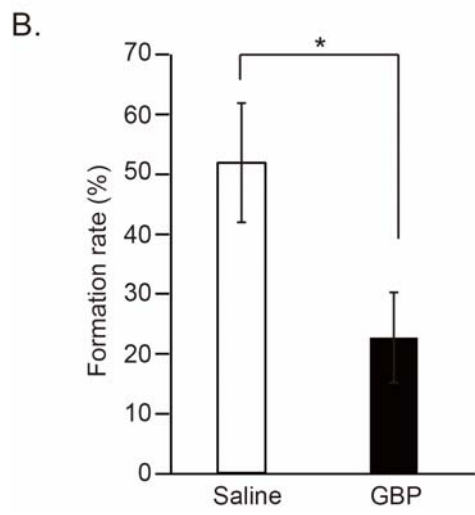
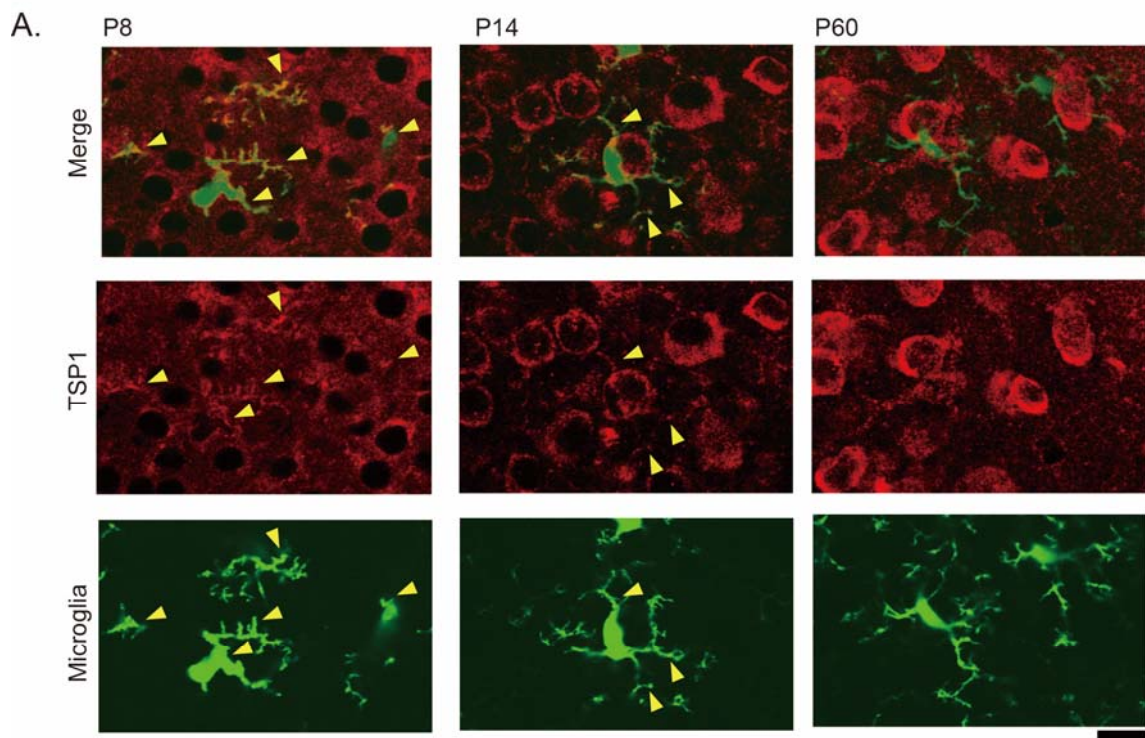
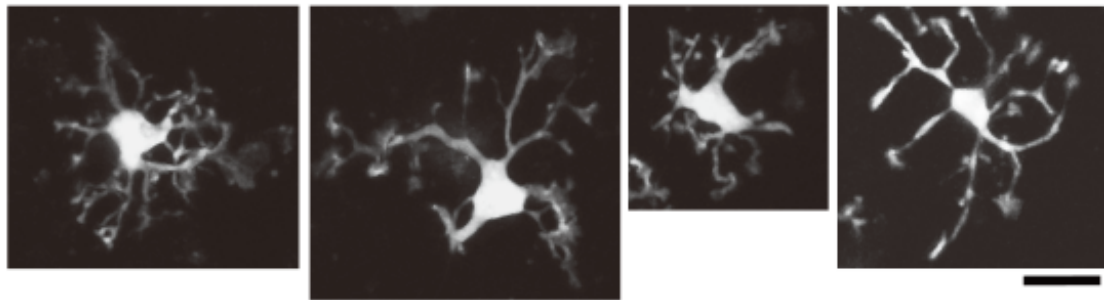


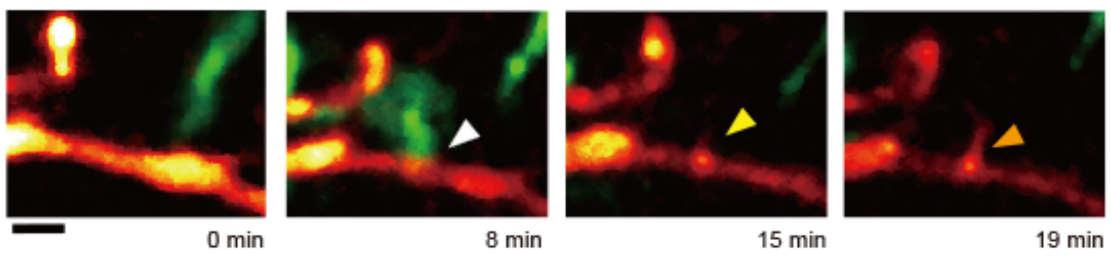
Figure 5. Accumulation of actin in dendrites following microglia contact

- A. Representative images of microglia in cortical slice culture at DIV 4. Slices were made from P5 Iba1-EGFP mice cortex. Scale bar 20 μm . Note the large soma and less extensive processes as compared to older *in vivo* microglia (Figure 3B) suggesting an activated-like phenotype.
- B. Typical time-lapse images showing actin (red) accumulation at dendrites and then filopodia following microglia (green) contact. White arrowhead shows microglia contact on to a dendrite, yellow arrowheads shows actin accumulation at the same region, followed by filopodia formation (orange arrowhead). Scale bar 5 μm .
- C. Relative fluorescence overlays of dendrite and adjacent regions showing time course of microglia contact and actin accumulation. The Green line represents microglia fluorescence on the dendrite. Blue line indicates intensity of lifeact-mCherry red fluorescence within the dendrite. Red line shows intensity of fluorescence in filopodia that protruded from the contacted region.

Figure 5



B.



C.

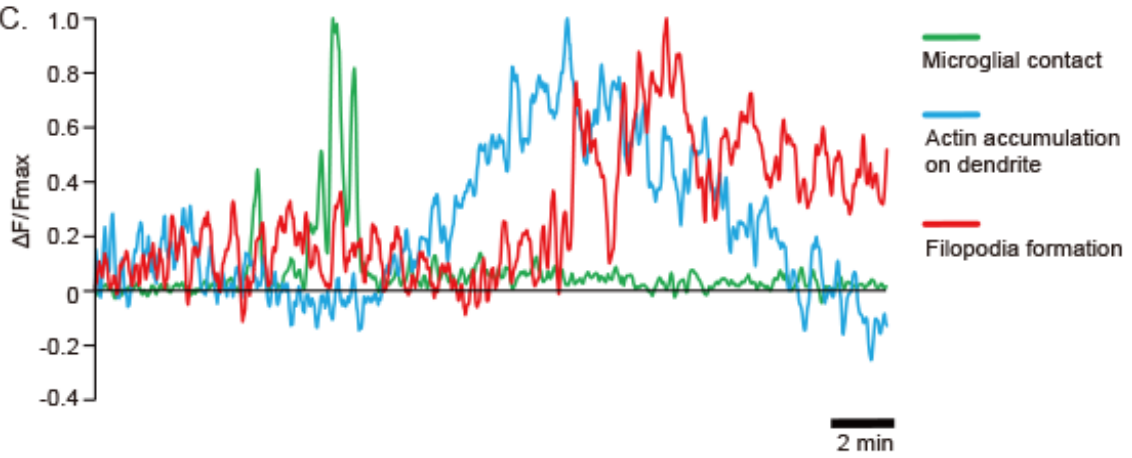


Figure 6. Spine density was decreased in minocycline injected mice.

- A. Representative images of basal dendrites of L2/3 pyramidal neurons from saline (top) and minocycline (bottom) injected mice. Minocycline or saline was injected daily between at P5-11, and mice were fixed at P11. Scale bar 5 μm .
- B. Spine density was significantly decreased in minocycline injected mice. $*p < 0.05$, unpaired t-test (Saline: animal n = 5, dendrite n = 157, Mino: animal n = 5, dendrite n = 210, Error bar: SE)

Figure 6

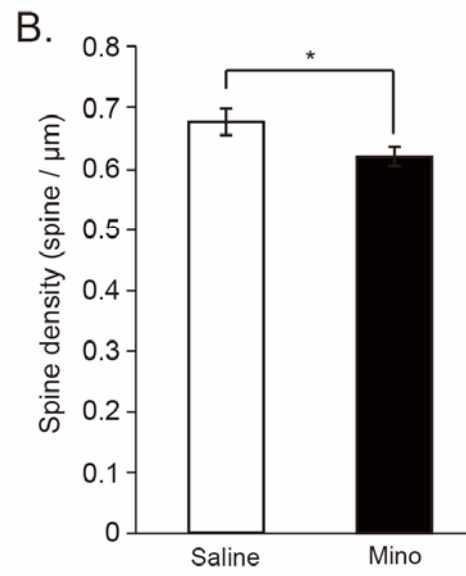
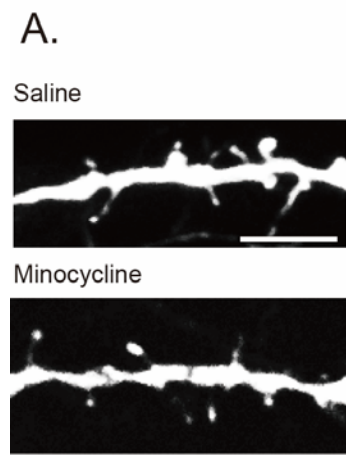


Figure 7. Spine density is decreased in microglia ablated mice.

- A. Representative images of microglia in sections of fixed somatosensory cortex from P8 control (Iba1-tTA) mice and from P8 Iba1-tTA::tetO-DTA mice following withdrawal of Dox from the diets of both mice from P5 to P8. Microglia were visualized using the anti-Iba1 antibody. Scale bar 50 μm .
- B. Average microglia density in control and microglia ablated mice, showing a significantly decrease of about 50 % in Iba1-tTA::tetO-DTA mice. *** $p < 0.01$, unpaired t-test (Control : n = 6 mice, DTA: n = 8 mice, Error bar: SEM)
- C. Representative images of basal dendrites of L2/3 pyramidal neurons from control and microglia ablated mice. Dox from the diets of both mice from P5 to P11 and mice were fixed at P11. Scale bar 5 μm .
- D. Average spine density in control and microglia ablated mice, showing a significantly decrease of about 50 % in Iba1-tTA::tetO-DTA mice. *** $p < 0.01$, unpaired t-test (Control: n = 7 mice, 104 dendrite, DTA: n = 4 mice, 109 dendrite, Error bar: SE)

Figure 7

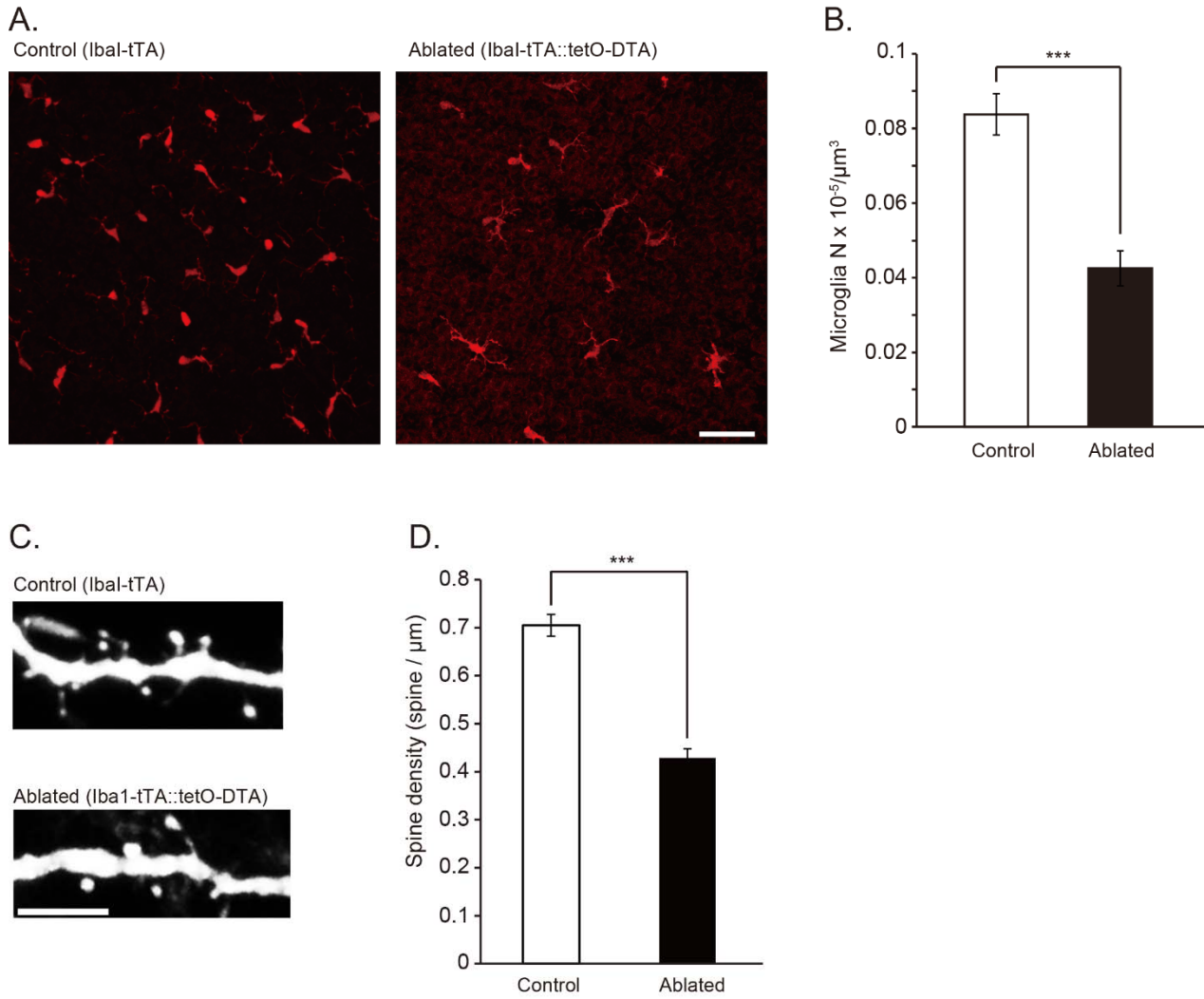
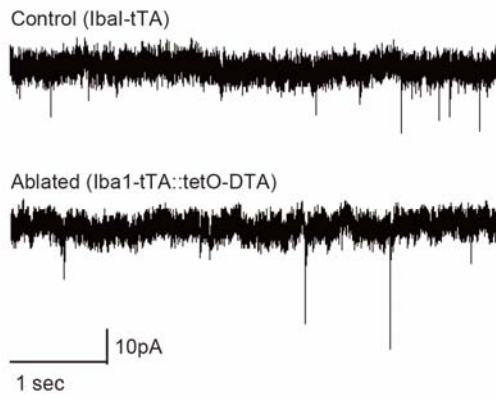


Figure 8. mEPSC frequency is decreased in microglia ablated mice.

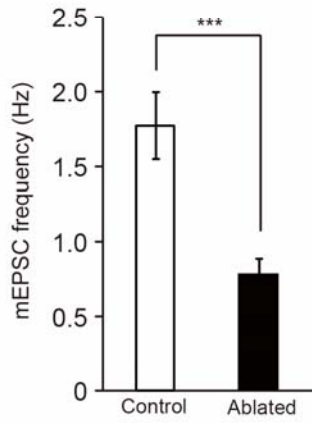
- A. Representative current traces recorded from L2/3 barrel cortex pyramidal neurons from control and microglia ablated mice. For this panel and for panel B and C, Dox was removed from the diet of both mice from P5 to P11 and recording were made at P12.
- B. Averaged mEPSC frequency (Bi) and cumulative frequency distribution curve (Bii) for control and microglia ablated mice. Microglia ablation significantly reduced mean mEPSC frequency ($***p < 0.01$, unpaired t-test).
- C. Averaged mEPSC amplitudes (Ci) and cumulative amplitude distribution curve (Cii) for control and microglia ablated mice. There was no significant difference in mean mEPSC amplitude. For data in panels B and C, control: n = 5 mice, n = 10 neurons, Ablated: n = 3 mice, n = 9 neurons, Error bar: SE)

Figure 8

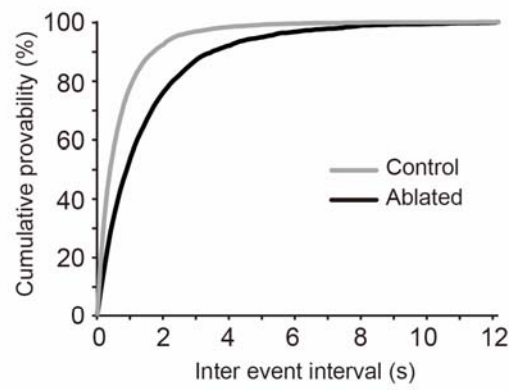
A.



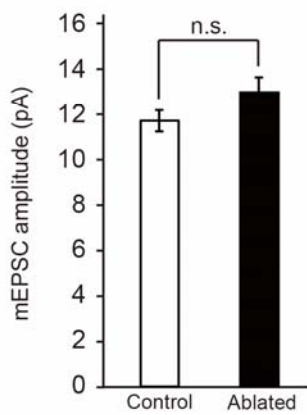
Bi.



Bii.



Ci.



Cii.

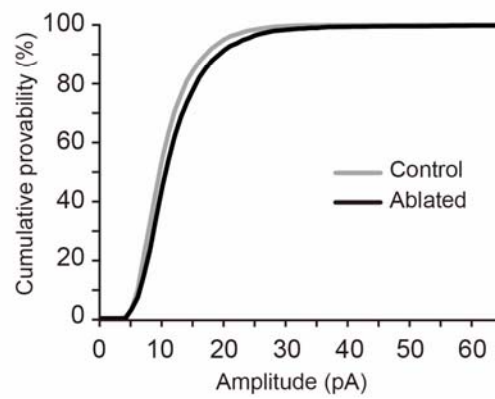


Figure 9. Comparison of microglia in intact and open-skull preparations

A. Representative images of microglia in fixed brain sections from intact Iba1-EGFP mice and from open-skull preparation Iba1-EGFP mice. Brains were fixed at P8-10.

Scale bar 20 μm .

B. Quantification of microglia morphological parameters in open-skull and control mice.

There was no significant differences in soma size (Bi), the number of primary process (B ii), nor in the total processes covered area (Biii). (Unpaired t-test, intact: n=14 cells, open skull: n=32 cells, Error bar: SE)

Figure 9

